

Provided for non-commercial research and education use.
Not for reproduction, distribution or commercial use.



This article appeared in a journal published by Elsevier. The attached copy is furnished to the author for internal non-commercial research and education use, including for instruction at the authors institution and sharing with colleagues.

Other uses, including reproduction and distribution, or selling or licensing copies, or posting to personal, institutional or third party websites are prohibited.

In most cases authors are permitted to post their version of the article (e.g. in Word or Tex form) to their personal website or institutional repository. Authors requiring further information regarding Elsevier's archiving and manuscript policies are encouraged to visit:

<http://www.elsevier.com/authorsrights>



Contents lists available at ScienceDirect

International Journal of Heat and Mass Transfer

journal homepage: www.elsevier.com/locate/ijhmt

Effective thermal conductivity of three-component composites containing spherical capsules

Alexander M. Thiele^a, Aditya Kumar^b, Gaurav Sant^{b,c}, Laurent Pilon^{a,*}^a Mechanical and Aerospace Engineering Department, Henry Samueli School of Engineering and Applied Science, University of California, Los Angeles, USA^b Civil and Environmental Engineering Department, Laboratory for the Chemistry of Construction Materials (LC²), Henry Samueli School of Engineering and Applied Science, University of California, Los Angeles, CA 90095, USA^c California Nanosystems Institute (CNSI), Los Angeles, CA 90095, USA

ARTICLE INFO

Article history:

Received 27 November 2013
 Received in revised form 25 January 2014
 Accepted 1 February 2014
 Available online 3 March 2014

Keywords:

Effective medium approximation
 Composite materials
 Three-phase media
 Phase change materials
 Microballoons
 Composite spheres

ABSTRACT

This paper presents detailed numerical simulations predicting the effective thermal conductivity of spherical monodisperse and polydisperse core-shell particles ordered or randomly distributed in a continuous matrix. First, the effective thermal conductivity of this three-component composite material was found to be independent of the capsule spatial distribution and size distribution. In fact, the study established that the effective thermal conductivity depended only on the core and shell volume fractions and on the core, shell, and matrix thermal conductivities. Second, the effective medium approximation reported by Felske (2004) [21] was in very good agreement with numerical predictions for any arbitrary combination of the above-mentioned parameters. These results can be used to design energy efficient composites, such as microencapsulated phase change materials in concrete and/or insulation materials for energy efficient buildings.

© 2014 Elsevier Ltd. All rights reserved.

1. Introduction

In 2010, building operations accounted for 41% of total US primary energy resource consumption [1]. Approximately, half of this energy was consumed for heating, ventilation, and air conditioning (HVAC) [1]. A common strategy to improve building energy efficiency is to use materials with a large thermal mass, e.g., concrete or brick [2,3]. While these materials can store large amounts of energy per unit mass, they operate passively, demonstrating only a sensible heat response [2,3]. To add an active or temperature sensitive dimension to the thermal behavior of building materials, there is interest in embedding phase change materials (PCMs) in building elements [4–7]. By reversibly undergoing solid–liquid phase transitions in relation to the temperature of their local environment, PCMs are able to actively and adaptively absorb and release latent heat required to induce phase transitions. These actions further enhance the thermal inertia of building systems. As such, if properly implemented, PCMs embedded in building materials can limit thermal exchange through exterior walls, reducing the need and cost for HVAC operations, and thus improving building energy efficiency.

The incorporation of PCMs (e.g., paraffin waxes, hydrated salts, or fatty acids) in building composites is facilitated by encapsulating the PCMs in a polymeric shell [6,5,4,7]. This serves to isolate the PCM from high pH chemical environments common to building materials, thus enhancing durability and limiting contamination [4–7]. When PCMs are embedded in a cementitious material, the resultant composite consists of three distinct components in the form of matrix (often cement-based), shell (often polymer-based), and PCM (often organic in nature). Clearly, this is a complex three-component composite material whose effective thermal properties must be predicted accurately to estimate heat transfer across composite building walls.

This study aims (1) to rigorously predict the effective thermal conductivity of three-component core-shell composite materials (2) to identify the controlling design parameters and (3) to derive design rules for composite walls. The results of this study could also be applicable to other multicomponent composites including self-healing microcapsule-doped polymers [8] and hollow glass microsphere-embedded syntactic foams [9], to name a few.

2. Background

Numerous models have been derived to predict the effective thermal conductivity of two-component composites as reviewed by Progelhof et al. [10], for example. Comparatively, few models

* Corresponding author. Tel.: +1 (310) 206 5598; fax: +1 (310) 206 2302.
 E-mail address: pilon@seas.ucla.edu (L. Pilon).

Nomenclature

A parameter in Eq. (4)
 A_c cross-sectional area, m^2
 B parameter in Eq. (4)
 C_D centroidal distance between two proximal capsules, μm
 D diameter, μm
 k thermal conductivity, $W/m K$
 L unit cell length, μm
 N number of unit cells
 \mathbf{n} normal unit vector
 p number of spherical capsules in a unit cell
 r radius, μm
 q''_x, q''_y, q''_z heat flux along the x -, y -, and z -directions, W/m^2
 \bar{q}''_x area-averaged heat flux along the x -direction, W/m^2
 t_s thickness of capsule shell, i.e. $t_s = (D_s - D_c)/2$, μm
 T temperature, K
 T_o, T_L temperature at $x = 0$ and $x = L$, K

Greek symbols

β parameter in Eq. (9)
 Δx minimum mesh size, μm

δ ratio of shell diameter to core diameter, $\delta = D_s/D_c$
 ϕ_i volume fraction of phase “ i ” in the composite structure
 $\phi_{c/s}$ volume fraction of core in the capsule,
 $\phi_{c/s} = \phi_c/(\phi_c + \phi_s)$
 ϕ_{c+s} volume fraction of capsules in the composite structure,
 $\phi_{c+s} = \phi_c + \phi_s$
 ϕ_{max} volume fraction of closely-packed capsules
 Θ_N, Θ_D numerator and denominator of the Felske model (Eq. (3))

Subscripts

c refers to core
 $c + s$ refers to core-shell particle
 cr refers to the critical thermal conductivity ratios
 eff refers to effective properties
 m refers to matrix
 s refers to shell

exist for three-component composites [11–21]. Several models were developed for liquid and gas phases in a porous solid matrix such as building materials or soil [17,18]. Other models require prior knowledge of the temperature gradients in each component of the composite to determine the effective thermal conductivity [13,14]. The most practical models provide explicit analytical expressions for the effective thermal conductivity of three-component composites based on the constituent thermal conductivities and on the geometric parameters of the composite structure such as core and shell diameters and/or volume fractions.

Lichtenecker [20] proposed an ad hoc expression for the electrical permittivity of a composite consisting of any number of randomly mixed components [22]. Woodside and Messmer [22], among others, have applied this model to the effective thermal conductivity of three-component composites expressed as [20,22,23],

$$k_{eff} = k_c^{\phi_c} k_s^{\phi_s} k_m^{\phi_m} \quad (1)$$

where k_c , k_s , and k_m are the thermal conductivities of the core, shell, and matrix materials, respectively. Similarly, ϕ_c , ϕ_s , and $\phi_m = 1 - \phi_c - \phi_s$, are the volume fractions of the core, shell, and matrix materials, respectively. Woodside and Messmer [22] referred to Eq. (1) as a “geometric mean” and noted that it corresponds to the arithmetic mean of the logarithms of the constituent thermal conductivities. Zakri et al. [23] analytically derived Lichtenecker’s [20] model (Eq. (1)) for the effective electrical permittivity of three-component composites. They concluded that Eq. (1) is “physically founded,” despite criticism from Reynolds and Hough [24] who suggested that the model “lacked a theoretical basis.” Note that Eq. (1) predicts that k_{eff} vanishes if the thermal conductivity of either the core or the shell vanishes. This is obviously not the case since heat conduction could still take place through the continuous matrix material.

Brailsford and Major [19] developed a model for the effective thermal conductivity of monodisperse homogeneous particles randomly distributed in a continuous matrix. This two-component model was equivalent to the Maxwell–Garnett model for electrical conductivity [25]. Brailsford and Major [19] extended the two-component model to account for monodisperse homogeneous particles made of two different materials randomly distributed in a continuous matrix. Then, the effective thermal conductivity of three-component media was given by [19],

$$k_{eff} = \frac{k_m \phi_m + k_c \phi_c \frac{3k_m}{(2k_m + k_c)} + k_s \phi_s \frac{3k_m}{(2k_m + k_s)}}{\phi_m + \phi_c \frac{3k_m}{(2k_m + k_c)} + \phi_s \frac{3k_m}{(2k_m + k_s)}} \quad (2)$$

Model predictions for two-component media agreed well with experimental data for the effective thermal conductivity of solid glass spheres surrounded by air or water [19]. However, experimental validation was not reported for three-component composite materials.

Felske [21] derived a model, using the self-consistent field approximation [26], to predict the effective thermal conductivity of monodisperse spherical capsules randomly distributed in a continuous matrix. This effort was motivated by the need to estimate the effective thermal conductivity of syntactic foam insulation. The geometry considered in the derivation consisted of a spherical volume of matrix material containing a concentric core-shell particle with volume fractions representative of the overall composite. The model accounted for contact resistance at the shell-matrix interface. An exact series solution of the heat conduction equation was obtained for the temperature distribution in each phase. In absence of contact resistance, the model can be expressed as [21],

$$k_{eff} = \frac{\Theta_N}{\Theta_D} k_m \quad (3)$$

Here, the numerator Θ_N and denominator Θ_D are expressed as [21],

$$\Theta_N = 2(1 - \phi_{c+s})A + (1 + 2\phi_{c+s})B \quad \text{and} \quad \Theta_D = (2 + \phi_{c+s})A + (1 - \phi_{c+s})B \quad (4)$$

where the parameters A and B are given by [21],

$$A = \left(1 + \frac{2}{\phi_{c/s}}\right) - \left(1 - \frac{1}{\phi_{c/s}}\right) \frac{k_c}{k_s} \quad \text{and} \quad B = \left(2 + \frac{1}{\phi_{c/s}}\right) \frac{k_c}{k_m} - 2 \left(1 - \frac{1}{\phi_{c/s}}\right) \frac{k_s}{k_m} \quad (5)$$

Here, ϕ_{c+s} is the volume fraction of the composite occupied by the capsule and $\phi_{c/s}$ is the volume fraction of the core with respect to the capsule. They are expressed as $\phi_{c+s} = (D_s/D_m)^3$ and $\phi_{c/s} = (D_c/D_s)^3$ where D_c , D_s , and D_m are the diameters of the core, shell, and matrix domains, respectively. The volume fraction of core-shell capsules ϕ_{c+s} can be written as $\phi_{c+s} = \phi_c + \phi_s$. Pal [12]

noted that the Felske model [21] “generally describes thermal conductivity data well when the core-shell volume fraction ϕ_{c+s} is less than about 0.2,” but no evidence was provided to demonstrate this claim.

Park et al. [11] also developed a model predicting the effective thermal conductivity of monodisperse spherical capsules randomly distributed in a continuous matrix based on a two-step approach. First, the effective thermal conductivity of the two-component core-shell capsule denoted by k_{c+s} was modeled based on the core and shell thermal conductivities and on the volume fraction of core with respect to the core-shell composite $\phi_{c/s}$. It was based on a modified Eshelby effective-medium approximation (EMA) [27,28] and expressed as [11],

$$k_{c+s} = \frac{2(1 - \phi_{c/s})k_s + (1 + 2\phi_{c/s})k_c}{(2 + \phi_{c/s})k_s + (1 - \phi_{c/s})k_c} k_s \quad (6)$$

The effective thermal conductivity k_{eff} of the three-component composite was then expressed based on the core-shell effective thermal conductivity k_{c+s} , the matrix thermal conductivity k_m , and the core-shell volume fraction ϕ_{c+s} as [11],

$$k_{eff} = \frac{2(1 - \phi_{c+s})k_m + (1 + 2\phi_{c+s})k_{c+s}}{(2 + \phi_{c+s})k_m + (1 - \phi_{c+s})k_{c+s}} k_m \quad (7)$$

After careful consideration, combining Eqs. (6) and (7) led to the Felske model [21] given by Eqs. (3)–(5).

Pal [12] developed an implicit model to predict the effective thermal conductivity of three-component composites of monodisperse spherical capsules randomly distributed in a continuous matrix. This model was derived using the differential effective medium approach [29]. The resulting model was an implicit function of the volume fraction of capsules expressed as [12],

$$\left(\frac{k_{eff}}{k_m}\right)^{1/3} \left(\frac{\beta - 1}{\beta - k_{eff}/k_m}\right) = \left(1 - \frac{\phi_{c+s}}{\phi_{c+s,max}}\right)^{-\phi_{c+s,max}} \quad (8)$$

where $\phi_{c+s,max}$ is the maximum capsule volume fraction for a given packing arrangement and β was expressed as [12],

$$\beta = \frac{(2 + \delta^3) \frac{k_c}{k_m} - 2(1 - \delta^3) \frac{k_s}{k_m}}{(1 + 2\delta^3) - (1 - \delta^3) \frac{k_c}{k_s}} \quad (9)$$

where δ is the shell to core diameter ratio, i.e., $\delta = D_s/D_c$ or $\delta^3 = \phi_{c/s}^{-1}$. The model accounted for the upper limit of the capsule volume fraction $\phi_{c+s,max}$ corresponding to close packing. Predictions by Eqs. (8) and (9) were reported to agree well with experimental data for thirteen different samples of two-phase media for “reasonable values” of $\phi_{c+s,max}$ [12]. However, $\phi_{c+s,max}$ was taken as 0.7, 0.85, or 1 which seems arbitrary and large. Indeed, the maximum volume fraction reaches 0.74 for face-centered cubic packing and 0.6 for randomly distributed monodisperse solid spheres [30]. Note that in the case of composite building materials with PCM, the capsule volume fraction is typically much smaller than the packing limit, as large volume fractions could compromise the mechanical strength of the wall [7].

Overall, several EMAs have been proposed in the literature for the effective thermal conductivity of three-component composite materials consisting of monodisperse capsules in a continuous matrix. However, these models are significantly different from one another and their validation against experimental data has been limited mainly to two-component media. Therefore, it remains unclear which one of these models is the most appropriate and accurate. In addition, to the best of our knowledge, no study has rigorously investigated the effects of the capsules’ spatial and size distributions on the effective thermal conductivity of three-component composites.

The aim of this study is to predict and to identify the dominant parameters controlling the effective thermal conductivity of three-component composite materials. To do so, detailed “numerical experiments” were performed to investigate the effects of (1) core and shell dimensions and volume fractions, (2) spatial distribution of the capsules, (3) size distribution of the capsules, and (4) core, shell, and matrix thermal conductivities. The results were compared with the previously reviewed EMAs to identify the most appropriate one and its range of validity.

3. Analysis

3.1. Schematics

The present study examined various composite representative volumes consisting of different packing arrangements of monodisperse and polydisperse spherical capsules distributed in a continuous matrix. Fig. 1 shows three-component unit cells with

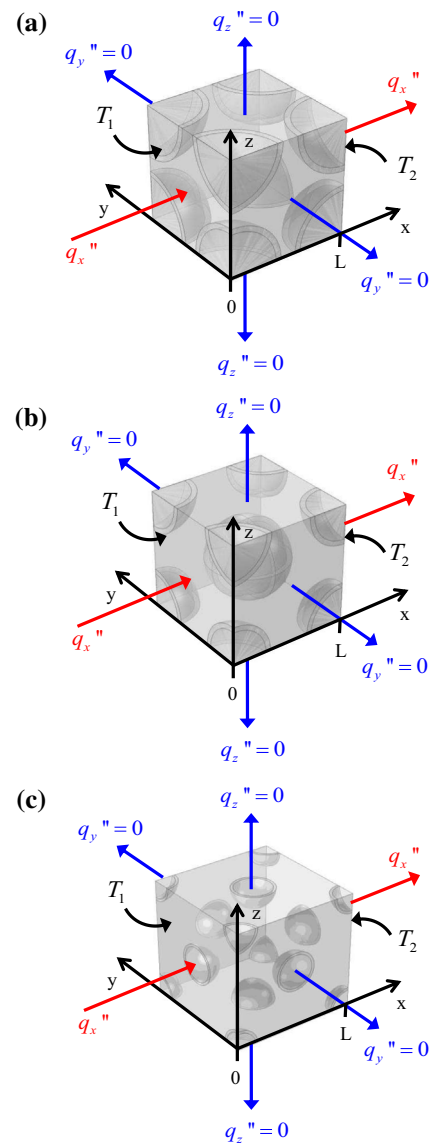


Fig. 1. Schematic and computational domain of a single unit cell consisting of capsules distributed in a continuous matrix with (a) simple, (b) body-centered, and (c) face-centered cubic packing arrangement. Core and shell diameters and unit cell length corresponding to core and shell volume fractions ϕ_c and ϕ_s were denoted by D_c , D_s , and L , respectively.

(a) simple, (b) body-centered, and (c) face-centered cubic packing arrangements along with the associated Cartesian coordinate system. The inner core and outer shell diameters were given by D_c and D_s , respectively with shell thickness $t_s = (D_s - D_c)/2$, and the length of the unit cell was denoted by L . For any packing arrangement of monodisperse capsules, the core and shell volume fractions ϕ_c and ϕ_s were expressed as,

$$\phi_c = \frac{p\pi D_c^3}{6L^3} \quad \text{and} \quad \phi_s = \frac{p\pi(D_s^3 - D_c^3)}{6L^3} \quad (10)$$

where p is the number of spherical capsules per unit cell. It was equal to 1, 2, and 4 for simple, body-centered, or face-centered cubic arrangements, respectively.

To study the effects of the capsule's size and spatial distributions in detail, a microstructural stochastic packing algorithm was implemented [31]. This algorithm considered a size distribution corresponding to an average outer shell diameter D_s of 18 μm with 10th and 95th percentile diameters equal to 9 μm and 33 μm , respectively, and a shell thickness t_s of 1 μm . It placed spherical capsules in a 3D representative volume of arbitrary size until the desired core phase volume fraction was achieved. Microstructural generation and packing was performed such that the minimum centroidal distance C_D between two proximal capsules was always greater than the sum of their radii r_1 and r_2 , i.e., $C_D > r_1 + r_2$. The packing algorithm placed capsules at random locations in the volume in accordance with two packing rules: (1) the size and number of capsules maintained the desired size distribution and (2) the desired core phase volume fraction was achieved within 0.5%. Fig. 2 shows examples of computational volumes consisting of 38 to 61 monodisperse or polydisperse capsules randomly distributed in a continuous matrix. Fig. 2(a)–(d) correspond to cases 3, 6, 9, and 10 summarized in Table 1, respectively.

3.2. Assumptions

To make the problem mathematically tractable, the following assumptions were made: (1) steady-state heat conduction

prevailed. (2) All materials were isotropic and had constant properties. (3) There was no heat generation. (4) Interfacial contact resistance was neglected, and (5) phase change and natural convection in the core phase were absent. This last assumption stemmed from the fact that even if microcapsules were filled with liquid (e.g. molten PCM) the Rayleigh number would be small.

3.3. Governing equations and boundary conditions

Under the above assumptions, the local temperatures in the core, shell, and matrix denoted by T_c , T_s , and T_m were governed by the steady-state heat diffusion equation in each domain, given by,

$$\nabla^2 T_c = 0, \quad \nabla^2 T_s = 0, \quad \text{and} \quad \nabla^2 T_m = 0 \quad (11)$$

These equations were coupled through the boundary conditions. Heat conduction took place mainly in the x -direction of the unit cell or representative cube (Figs. 1 or 2) by imposing the temperature on the faces of the cube located at $x = 0$ and $x = L$ such that for $0 \leq y \leq L$ and $0 \leq z \leq L$,

$$T(0, y, z) = T_o \quad \text{and} \quad T(L, y, z) = T_L \quad (12)$$

By virtue of symmetry, the heat flux through the four lateral faces vanished, i.e.,

$$q''_y(x, 0, z) = q''_y(x, L, z) = 0 \quad \text{and} \quad q''_z(x, y, 0) = q''_z(x, y, L) = 0 \quad (13)$$

where $q''_y(x, y, z)$ and $q''_z(x, y, z)$ are the heat fluxes along the y - and z -axes, respectively. They are given by Fourier's law, i.e., $q''_y = -k\partial T/\partial y$ and $q''_z = -k\partial T/\partial z$. The boundary temperatures on the faces $x = 0$ and $x = L$ were taken as $T_o = 294$ K and $T_L = 292$ K. Coupling between the temperatures of the different domains was achieved by imposing continuous heat flux across their interfaces, i.e.,

$$-k_m \frac{\partial T_m}{\partial \mathbf{n}} \Big|_{m/s} = -k_s \frac{\partial T_s}{\partial \mathbf{n}} \Big|_{m/s} \quad \text{and} \quad -k_s \frac{\partial T_s}{\partial \mathbf{n}} \Big|_{s/c} = -k_c \frac{\partial T_c}{\partial \mathbf{n}} \Big|_{s/c} \quad (14)$$

where \mathbf{n} is the unit normal vector at any given point on the matrix/shell and shell/core interfaces, designated by subscript m/s and s/c , respectively.

3.4. Data processing

Based on Fourier's law, the effective thermal conductivity of the core-shell composite medium was computed from the imposed temperature difference along the x -direction, the domain length L , and the area-averaged heat flux \bar{q}''_x along the x -direction according to,

$$k_{\text{eff}} = -\frac{\bar{q}''_x L}{T_L - T_o} \quad \text{where} \quad \bar{q}''_x(x) = \frac{1}{A_c} \iint q''_x(x, y, z) dy dz \quad (15)$$

Here, A_c is the cross-sectional area of the computational domain perpendicular to the x -axis. Due to the heterogeneous nature of the composite medium the heat flux was not uniform over a given cross-section perpendicular to the x -axis. However, it was systematically verified that the area-averaged heat flux $\bar{q}''_x(x)$ was the same at any cross-section between $x = 0$ and $x = L$.

3.5. Method of solution

The governing equation (11) along with the boundary conditions given by Eqs. (12)–(14) were solved using finite element methods. The numerical convergence criteria was defined such that the maximum relative difference in the predicted local area-averaged heat flux $\bar{q}''_x(x)$ was less than 0.5% when reducing the mesh size by a factor of 2. Converged solutions were obtained by

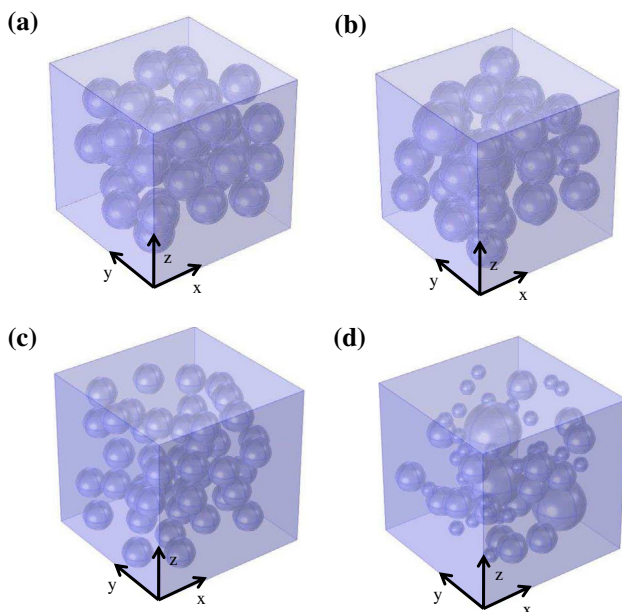


Fig. 2. Computational cells containing monodisperse capsules with (a) $p = 39$, $L = 75 \mu\text{m}$, $\phi_c = 0.198$, and $\phi_s = 0.041$, and (c) $p = 49$, $L = 100 \mu\text{m}$, $\phi_c = 0.105$, and $\phi_s = 0.045$, as well as polydisperse capsules with (b) $p = 38$, $L = 75 \mu\text{m}$, $\phi_c = 0.197$, and $\phi_s = 0.075$, and (d) $p = 61$, $L = 100 \mu\text{m}$, $\phi_c = 0.095$, and $\phi_s = 0.035$.

Table 1

Numerical and analytical predictions of the effective thermal conductivity of composites consisting of monodisperse or polydisperse capsules randomly distributed in a continuous matrix. The average outer diameter and thickness of the shell are $D_{s,avg} = 18 \mu\text{m}$ and $t_s = 1 \mu\text{m}$, respectively for all cases.

	Size distribution	Input						Numerical k_{eff} (W/m K)	Eq. (17) k_{eff} (W/m K)	% Difference	
		p	L (μm)	ϕ_c	ϕ_s	k_c (W/m K)	k_s (W/m K)				k_m (W/m K)
1	Monodisperse	19	75	0.097	0.041	0.21	1.3	0.4	0.41	0.41	0.02
2	Polydisperse	22	75	0.095	0.041	0.21	1.3	0.4	0.41	0.41	0.02
3	Monodisperse	39	75	0.198	0.084	0.21	1.3	0.4	0.42	0.42	0.01
4	Monodisperse	39	75	0.198	0.084	10	100	30	30.17	30.17	0.00
5	Monodisperse	39	75	0.198	0.084	100	10	30	33.41	33.42	0.03
6	Polydisperse	38	75	0.197	0.075	0.21	1.3	0.4	0.41	0.41	0.11
7	Polydisperse	38	75	0.197	0.075	10	100	30	29.68	29.72	0.14
8	Polydisperse	38	75	0.197	0.075	100	10	30	33.85	33.78	0.22
9	Monodisperse	49	100	0.105	0.045	10	20	50	42.83	42.89	0.14
10	Polydisperse	61	100	0.095	0.035	50	10	20	21.30	21.28	0.10

imposing the minimum mesh size to be $\Delta x = (D_s - D_c)/4$ and the maximum growth rate to be 1.5. The number of finite elements needed to obtain a converged solution ranged from 12,873 to 1,451,237 depending on the size of the computational cell and on the core and shell dimensions.

In order to validate the computational tool, a unit cell containing capsules with face-centered cubic packing arrangement was simulated with the same boundary conditions given by Eqs. (12)–(14) but assuming $k_s = k_c = k_m$. As expected, the predicted area-averaged heat flux at $x = L$ fell within 0.5% of Fourier's law given by $\bar{q}_x''(x) = k_m(T_o - T_L)/L$ for $L = 20.3 \mu\text{m}$, $k_m = 0.4 \text{ W/m K}$, $T_o = 294 \text{ K}$, and $T_L = 292 \text{ K}$. Note also that the area-averaged heat flux $\bar{q}_x''(x)$ was the same at any cross-section along the x -direction.

4. Results and discussion

4.1. Effect of capsule dimensions and packing arrangement

Fig. 3 shows the effective thermal conductivity k_{eff} for domains comprised of 1 to 20 stacked unit cells for simple, body-centered, and face-centered cubic packing arrangements (Fig. 1). Two sets of volume fractions were considered: (i) $\phi_c = 0.25$ and $\phi_s = 0.1$ and (ii) $\phi_c = 0.05$ and $\phi_s = 0.0165$. The diameters D_c and D_s and the unit cell length L were adjusted with each packing arrangement to achieve the desired volume fractions. The core, shell, and matrix thermal conductivities were taken to be $k_c = 0.21 \text{ W/m K}$

[32], $k_s = 1.3 \text{ W/m K}$ [33], and $k_m = 0.4 \text{ W/m K}$ [34], respectively. These values correspond to paraffin wax PCM in silica shells embedded in cement. Fig. 3 establishes that k_{eff} was independent (i) of the number of stacked unit cells, as expected from symmetry considerations, and (ii) of the choice of packing arrangement. The same conclusions were reached for different volume fractions. Therefore, a single unit cell with a face-centered cubic packing arrangement will be considered in the remainder of this study as

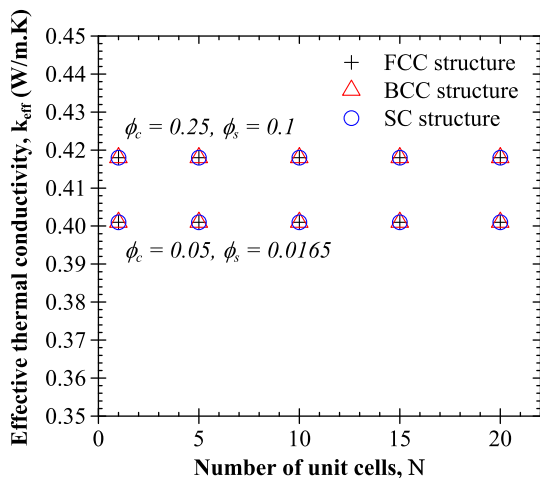


Fig. 3. Effective thermal conductivity for linear arrays of N unit cells with two different combinations of volume fractions ϕ_c and ϕ_s and packing arrangements SC, BCC, and FCC. Core, shell, and matrix thermal conductivities were $k_c = 0.21 \text{ W/m K}$, $k_s = 1.3 \text{ W/m K}$, and $k_m = 0.4 \text{ W/m K}$, respectively.

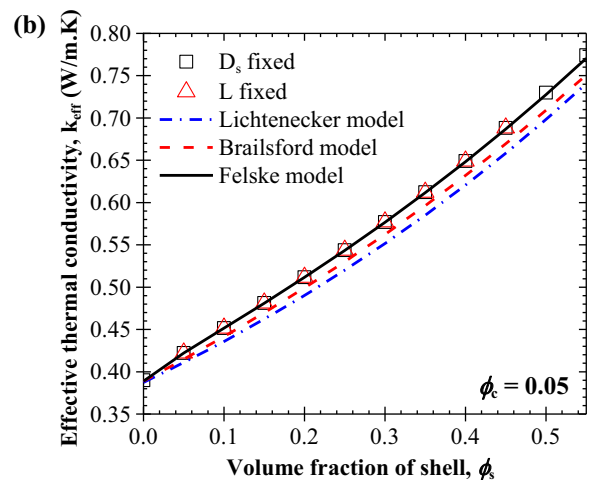
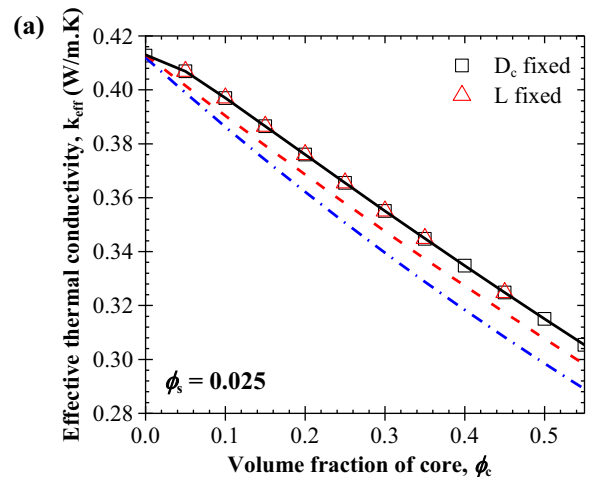


Fig. 4. Effective thermal conductivity for (a) different values of ϕ_c with $\phi_s = 0.025$ and (b) different values of ϕ_s with $\phi_c = 0.05$. The volume fractions were varied by adjusting either the diameter or unit cell length. Here, $k_c = 0.21 \text{ W/m K}$, $k_s = 1.3 \text{ W/m K}$, and $k_m = 0.4 \text{ W/m K}$. Predictions by the Lichtenecker, Brailsford, and Felske models are also shown.

representative of any composite media consisting of ordered monodisperse capsules.

Fig. 4 shows the effective thermal conductivity k_{eff} of a composite containing monodisperse capsules as a function of (a) the core volume fraction ϕ_c ranging from 0.0 to 0.55 for a constant shell volume fraction of $\phi_s = 0.025$ and (b) the shell volume fraction ϕ_s ranging from 0.0 to 0.55 for a constant core volume fraction of $\phi_c = 0.05$. The desired volume fractions were imposed by either adjusting the relevant diameter (D_c or D_s) while holding the unit cell length L constant or by adjusting the unit cell length L and holding the relevant diameter constant. Here also, the core, shell, and matrix thermal conductivities were taken as $k_c = 0.21$ W/m K, $k_s = 1.3$ W/m K, and $k_m = 0.4$ W/m K, respectively. Fig. 4(a) and (b) establish that k_{eff} depended only on ϕ_c and ϕ_s and not on the individual geometric parameters D_c , D_s , and L .

Overall, this section demonstrated that the effective thermal conductivity of a composite material containing monodisperse capsules was a function only of five parameters namely, the volume fractions ϕ_c and ϕ_s and the constituent material thermal conductivities k_c , k_s , and k_m , i.e., $k_{eff} = k_{eff}(\phi_c, \phi_s, k_c, k_s, k_m)$.

4.2. Effect of core and shell volume fractions

For any packing arrangement of monodisperse spherical capsules the term $\phi_{c/s}$ used in Eqs. (5) and (6) can be written in terms of ϕ_c and ϕ_s so that,

$$\frac{1}{\phi_{c/s}} = 1 + \frac{\phi_c}{\phi_s} \quad (16)$$

Then, the Felske model [21], given by Eq. (3) can be written in terms of ϕ_c and ϕ_s as,

$$k_{eff} = \frac{2k_m(1 - \phi_c - \phi_s) \left(3 + 2\frac{\phi_c}{\phi_c} + \frac{\phi_s k_c}{\phi_c k_s} \right) + (1 + 2\phi_c + 2\phi_s) \left[\left(3 + \frac{\phi_s}{\phi_c} \right) k_c + 2\frac{\phi_s k_c}{\phi_c} \right]}{(2 + \phi_c + \phi_s) \left(3 + 2\frac{\phi_s}{\phi_c} + \frac{\phi_c k_c}{\phi_c k_s} \right) + (1 - \phi_c - \phi_s) \left[\left(3 + \frac{\phi_c}{\phi_c} \right) \frac{k_c}{k_m} + 2\frac{\phi_c k_c}{\phi_c k_m} \right]} \quad (17)$$

Similar operation can also be performed for the models proposed by Park [11] and Pal [12]. Thus, the EMAs previously reviewed satisfy the relationship $k_{eff} = k_{eff}(\phi_c, \phi_s, k_c, k_s, k_m)$. However, it remains unclear which one accurately predicts the effective thermal conductivity retrieved from detailed numerical simulations based on Eq. (15).

Fig. 4 compares the effective thermal conductivity k_{eff} of a composite containing monodisperse capsules retrieved numerically with that predicted by the Lichtenecker [20], Brailsford [19], and Felske [21] models given respectively by Eqs. (1), (2), and (17) as a function of (a) the core volume fraction ϕ_c for $\phi_s = 0.025$ and (b) the shell volume fraction ϕ_s for $\phi_c = 0.05$. Here also, $k_c = 0.21$ W/m K, $k_s = 1.3$ W/m K, and $k_m = 0.4$ W/m K, respectively. Fig. 4(a) and (b) indicate that k_{eff} decreased as ϕ_c increased and increased as ϕ_s increased, for the values of k_c , k_s , and k_m considered. More importantly, they indicate that predictions by the Felske model (Eq. (17)) fell within 0.5% of numerical predictions, i.e., within numerical uncertainty. The other models underpredicted k_{eff} by 2.4% to 5.4% for the values of ϕ_c , ϕ_s , k_c , k_s , and k_m considered. These relative errors are expected to increase as the thermal conductivity mismatch between the three phases increases.

4.3. Effect of constituent thermal conductivities

Fig. 5 plots the effective thermal conductivity k_{eff} of a composite material containing monodisperse capsules as a function of matrix thermal conductivity k_m ranging from 1 to 50 W/m K for volume fractions $\phi_c = 0.2$ and $\phi_s = 0.145$ and two combinations of core and shell thermal conductivities, namely, (i) $k_c = 5$ W/m K and

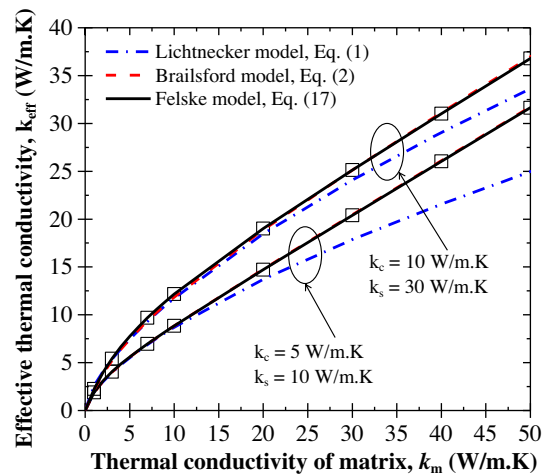


Fig. 5. Effective thermal conductivity k_{eff} of core-shell composite as a function of the thermal conductivity of the continuous phase k_m obtained numerically and predicted by the Lichtenecker, Brailsford, and Felske models given by Eqs. (1), (2) and (17), respectively. The volume fractions of core and shell were $\phi_c = 0.2$ and $\phi_s = 0.145$.

$k_s = 10$ W/m K and (ii) $k_c = 10$ W/m K and $k_s = 30$ W/m K. This study demonstrated that predictions of k_{eff} by the Felske model (Eq. (17)) fell within 0.3% of the numerical predictions for k_m up to 500 W/m K (see supplementary material). On the other hand, predictions by the Brailsford model (Eq. (2)) and the Lichtenecker model (Eq. (1)) underpredicted k_{eff} by up to 3% and 60%, respectively. The discrepancies between these model's predictions and numerical simulations increased with increasing k_m .

Fig. 6 plots the effective thermal conductivity k_{eff} of a composite containing monodisperse capsules as a function of the core thermal conductivity k_c ranging from 1 to 500 W/m K for volume fractions $\phi_c = 0.2$ and $\phi_s = 0.145$ and two combinations of matrix and shell thermal conductivities, namely, (i) $k_m = 5$ W/m K and $k_s = 10$ W/m K and (ii) $k_m = 10$ W/m K and $k_s = 30$ W/m K. Fig. 6 demonstrates that predictions by the Felske model (Eq. (17)) fell within 0.2% of the numerical predictions while the other models deviated by more than 10% for the values of k_m and k_s considered. Fig. 6 also indicates that k_{eff} asymptotically reached a plateau as k_c increased. This can be attributed to the fact that as k_c becomes

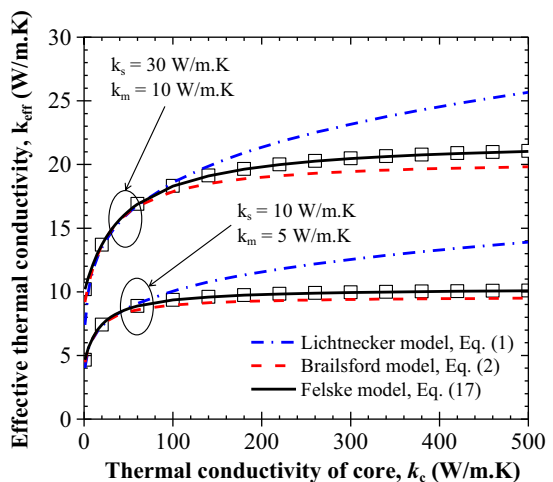


Fig. 6. Effective thermal conductivity k_{eff} of core-shell composite as a function of the thermal conductivity of the core phase k_c obtained numerically and predicted by the Lichtenecker, Brailsford, and Felske models given by Eqs. (1), (2) and (17), respectively. The volume fractions of core and shell were $\phi_c = 0.2$ and $\phi_s = 0.145$.

much greater than k_s and k_m , the temperature gradient throughout the core material vanishes. Then, the core provides negligible thermal resistance to heat conduction through the composite medium and thus does not affect k_{eff} . From a mathematical point of view, for $k_c \gg k_s$ and $k_c \gg k_m$, Eq. (17) simplifies to

$$k_{eff} = \frac{2(1 - \phi_c - \phi_s) \frac{\phi_s k_m}{\phi_c k_s} + (1 + 2\phi_c + 2\phi_s) \left(3 + \frac{\phi_s}{\phi_c}\right)}{(2 + \phi_c + \phi_s) \frac{\phi_s}{\phi_c k_s} + (1 - \phi_c - \phi_s) \left(3 + \frac{\phi_s}{\phi_c}\right) \frac{1}{k_m}} \quad (18)$$

Similarly, Fig. 7 plots the effective thermal conductivity k_{eff} of a composite material containing monodisperse capsules as a function of shell thermal conductivity k_s ranging from 1 to 500 W/m K for volume fractions $\phi_c = 0.2$ and $\phi_s = 0.145$ and two combinations of core and matrix thermal conductivities, namely, (i) $k_c = 5$ W/m K and $k_m = 10$ W/m K and (ii) $k_c = 10$ W/m K and $k_m = 30$ W/m K. Here also, the Felske model [Eq. (17)] agreed very well with the numerical predictions while the other models deviated by more than 33% for the values of k_c and k_m considered. For $k_s \gg k_c$ and $k_s \gg k_m$, k_{eff} asymptotically converged to a function independent not only of k_s but also of k_c given by,

$$k_{eff} = \frac{(1 + 2\phi_c + 2\phi_s) k_m}{(1 - \phi_c - \phi_s)} \quad (19)$$

In this case, k_s did not contribute to k_{eff} because the shell thermal resistance was negligible compared with that of the matrix. In addition, heat can be transferred through the capsule via two paths: through the shell and the core, or along the shell around the core. When $k_s \gg k_c$ and $k_s \gg k_m$, the latter path provided the least resistance to heat transfer. Then, the highly conducting shell thermally “short-circuited” the core and k_c did not affect k_{eff} . As a result, k_{eff} was only a function of k_m .

Finally, Figs. 5–7 show that the Felske model (Eq. (17)) predicted the effective thermal conductivity of composites containing monodisperse capsules within the estimated numerical uncertainty for all volume fractions ϕ_c and ϕ_s considered and for a wide range of thermal conductivities k_s , k_c , and k_m . It remains to be shown whether this model is also valid for polydisperse and/or randomly distributed capsules.

4.4. Effect of capsule spatial and size distributions

Ten composite structures consisting of monodisperse and polydisperse microcapsules randomly distributed in a continuous

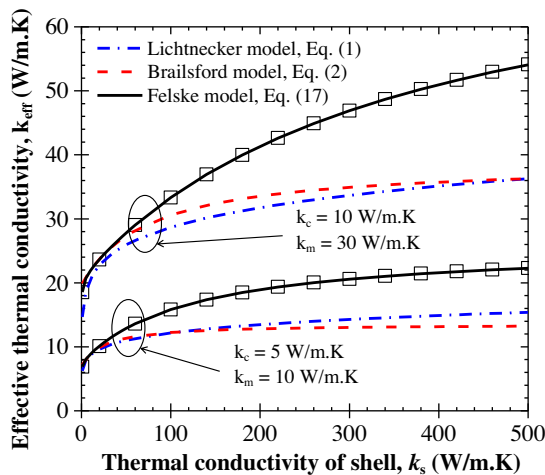


Fig. 7. Effective thermal conductivity k_{eff} of core–shell composite as a function of the thermal conductivity of the shell phase k_s obtained numerically and predicted by the Lichtnecker, Brailsford, and Felske models given by Eqs. (1), (2) and (17), respectively. The volume fractions of core and shell were $\phi_c = 0.2$ and $\phi_s = 0.145$.

matrix were generated as described previously. The number of capsules p in the computational domain ranged from 19 to 61 and the thickness of the shell was taken as $t_s = 1 \mu\text{m}$. Table 1 summarizes the different values of p , L , ϕ_c , ϕ_s , k_c , k_s , and k_m considered in each case. It also compares the numerically predicted effective thermal conductivity k_{eff} of these composite microstructures to that predicted by the Felske model (Eq. (17)). Cases 1 and 2 indicate that the numerically predicted k_{eff} was the same for composites with monodisperse or polydisperse capsules for the same values of ϕ_c , ϕ_s , k_c , k_s , and k_m . Table 1 also shows that k_{eff} predicted by the Felske model (Eq. (17)) fell within 0.25% of numerical predictions for a wide range of constituent thermal conductivities k_c , k_s , and k_m and volume fractions ϕ_c and ϕ_s .

In summary, these results established that the effective thermal conductivity of three-component composites consisting of capsules distributed in a continuous matrix was independent of capsule size distribution and of their spatial distribution. In all cases, the Felske model (Eq. (17)) predicted the effective thermal conductivity within numerical uncertainty.

4.5. Critical condition for effective thermal conductivity

As previously mentioned, encapsulated PCM can be used to reduce and delay the thermal load in concrete buildings. However, the addition of PCM microcapsules should not increase the effective thermal conductivity k_{eff} of the composite wall meant to provide not only large thermal mass but also act as thermal insulation [7]. Based on Eq. (17), the critical core to matrix thermal conductivity ratio above which k_{eff} becomes larger than k_m can be written as,

$$\left(\frac{k_c}{k_m}\right)_{cr} = \frac{2\left(\frac{k_s}{k_m} - 1\right) - 3\frac{\phi_c}{\phi_s}}{\frac{k_m}{k_s} - 1 - 3\frac{\phi_c}{\phi_s}} \quad (20)$$

This expression can be used as a thermal design rule for core–shell composite materials with monodisperse or polydisperse and ordered or randomly distributed capsules.

Fig. 8 plots the critical core to matrix thermal conductivity ratio $(k_c/k_m)_{cr}$ given by Eq. (20) as a function of the shell to matrix thermal conductivity ratio k_s/k_m . Four combinations of core and shell volume fractions were used, namely, (i) $\phi_c = 0.4$ and $\phi_s = 0.191$, (ii) $\phi_c = 0.2$ and $\phi_s = 0.124$, (iii) $\phi_c = 0.1$ and $\phi_s = 0.082$, and (iv) $\phi_c = 0.05$ and $\phi_s = 0.054$. All curves passed through the same point (1, 1) corresponding to $k_c = k_s = k_m = k_{eff}$. Each design curve represents the ensemble of conditions for which $k_{eff} = k_m$. The area

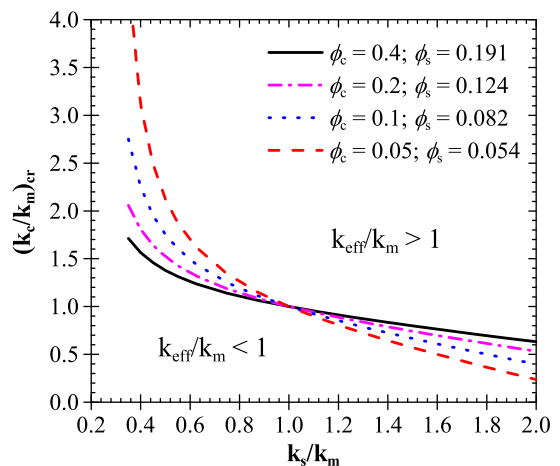


Fig. 8. Critical core and shell conductivity ratios $(k_c/k_m)_{cr}$ and (k_s/k_m) (a) for different values of matrix thermal conductivity k_m with $\phi_c = 0.4$ and $\phi_s = 0.191$ and (b) for core and shell volume fractions ϕ_c and ϕ_s .

under the curve correspond to the desirable conditions for which k_{eff} is smaller than k_m .

4.6. Comparison with experimental data

Several studies have experimentally measured the effective thermal conductivity of three-component core-shell composite materials [35–40]. Liang and Li [35] measured the effective thermal conductivity of polydisperse hollow glass microspheres randomly distributed in a polypropylene matrix. These measurements were then compared with numerical predictions using finite element methods [36]. Surprisingly, the measured effective thermal conductivity was larger than that of the individual constituent materials which cast doubt on the data. Other studies reported the effective thermal conductivity of three-component composites but did not report the thermal conductivities of the constituents and/or the relevant geometric parameters such as the shell and/or the core volume fractions [37–40]. However, these parameters are necessary in order to accurately validate numerical predictions and effective medium approximations. In addition, contact resistance between the different phases may affect the experimental measurements. This effect was considered in the general case of the Felske model [21].

5. Conclusion

This study established that the effective thermal conductivity was independent of the capsules' spatial distribution and size distribution. The effective thermal conductivity was found to depend solely on the core and shell volume fractions and on the core, shell, and matrix thermal conductivities. The Felske model (Eq. (17)) predicted the effective thermal conductivity of the composite material within numerical uncertainty for the wide range of parameters considered. This model was used to identify conditions under which the effective thermal conductivity k_{eff} of the composite materials remained smaller than that of the matrix material. This thermal design rule will be useful in developing PCM-composite materials for energy efficient buildings.

Acknowledgments

This report was prepared as a result of work sponsored by the California Energy Commission (Contract: PIR-12-032), the National Science Foundation (CMMI: 1130028) and the University of California, Los Angeles (UCLA). It does not necessarily represent the views of the Energy Commission, its employees, the State of California, or the National Science Foundation. The Energy Commission, the State of California, its employees, contractors, and subcontractors make no warranty, express or implied, and assume no legal liability for the information in this document; nor does any party represent that the use of this information will not infringe upon privately owned rights. This report has not been approved or disapproved by the California Energy Commission nor has the California Energy Commission passed upon the accuracy or adequacy of the information in this report.

Appendix A. Supplementary data

Supplementary data associated with this article can be found, in the online version, at <http://dx.doi.org/10.1016/j.ijheatmasstransfer.2014.02.002>.

References

- [1] US Department of Energy, Buildings energy data book. <<http://buildingsdatabook.eren.doe.gov>>, 2011.
- [2] C.A. Balaras, The role of thermal mass on the cooling load of buildings. An overview of computational methods, *Energy Build.* 24 (1) (1996) 1–10.
- [3] S.A. Kalogirou, G. Florides, S. Tassou, Energy analysis of buildings employing thermal mass in Cyprus, *Renewable Energy* 27 (3) (2002) 353–368.
- [4] M.M. Farid, A.M. Khudhair, S.A.K. Razack, S. Al-Hallaj, A review on phase change energy storage: materials and applications, *Energy Convers. Manage.* 45 (9) (2004) 1597–1615.
- [5] P.B. Salunke, P.S. Shembekar, A review on effect of phase change material encapsulation on the thermal performance of a system, *Renewable Sustainable Energy Rev.* 16 (8) (2012) 5603–5616.
- [6] A. Jayalath, P. Mendis, G. Gammampila, L. Aye, T. Ngo, Applications of phase change materials in concrete for sustainable built environment: a review, in: *International Conference on Structural Engineering, Construction, and Management (ICSECM)*, Kandy, Sri Lanka, December 16–18, 2011, pp. 1–13.
- [7] T.-C. Ling, C.-S. Poon, Use of phase change materials for thermal energy storage in concrete: an overview, *Constr. Build. Mater.* 46 (2013) 55–62.
- [8] E.N. Brown, S.R. White, N.R. Sottos, Microcapsule induced toughening in a self-healing polymer composite, *J. Mater. Sci.* 39 (5) (2004) 1703–1710.
- [9] V.V. Budov, Hollow glass microspheres. Use, properties, and technology (review), *Glass Ceram.* 51 (7) (1994) 230–235.
- [10] R.C. Progelhof, J.L. Throne, R.R. Ruetsch, Methods for predicting the thermal conductivity of composite systems: a review, *Polym. Eng. Sci.* 16 (9) (1976) 615–625.
- [11] Y.K. Park, J.-G. Kim, J.-K. Lee, Prediction of thermal conductivity of composites with spherical microballoons, *Mater. Trans.* 49 (12) (2008) 2781–2785.
- [12] R. Pal, Thermal conductivity of three-component composites of core-shell particles, *Mater. Sci. Eng. A* 498 (12) (2008) 135–141.
- [13] G.R. Hadley, Thermal conductivity of packed metal powders, *Int. J. Heat Mass Transfer* 29 (6) (1986) 909–920.
- [14] L.S. Verma, A.K. Shrotriya, R. Singh, D.R. Chaudhary, Prediction and measurement of effective thermal conductivity of three-phase systems, *J. Phys. D: Appl. Phys.* 24 (9) (1991) 1515–1526.
- [15] S.C. Cheng, R.I. Vachon, The prediction of the thermal conductivity of two and three phase solid heterogeneous mixtures, *Int. J. Heat Mass Transfer* 12 (3) (1969) 249–264.
- [16] D.R. Chaudhary, R.C. Bhandari, Heat transfer through a three-phase porous medium, *J. Phys. D: Appl. Phys.* 1 (6) (1968) 815–817.
- [17] Z. Pavlík, E. Vejmelková, L. Fiala, R. Černý, Effect of moisture on thermal conductivity of lime-based composites, *Int. J. Thermophys.* 30 (6) (2009) 1999–2014.
- [18] J. Kou, Y. Liu, F. Wu, J. Fan, H. Lu, Y. Xu, Fractal analysis of effective thermal conductivity for three-phase (unsaturated) porous media, *J. Appl. Phys.* 106 (5) (2009) 054905-1–054905-6.
- [19] A.D. Brailsford, K.G. Major, The thermal conductivity of aggregates of several phases, including porous materials, *Br. J. Appl. Phys.* 15 (1964) 313–319.
- [20] K. Lichtenecker, "Die dielektrizitätskonstante natürlicher und künstlicher mischkörper", *Phys. Z.* 27 (1926) 115–158.
- [21] J.D. Felske, Effective thermal conductivity of composite spheres in a continuous medium with contact resistance, *Int. J. Heat Mass Transfer* 47 (2004) 3453–3461.
- [22] W. Woodside, J.H. Messmer, Thermal conductivity of porous media. I. Unconsolidated sands, *J. Appl. Phys.* 32 (9) (1961) 1688–1699.
- [23] T. Zakri, J.-P. Laurent, M. Vauclin, Theoretical evidence for 'Lichtenecker's mixture formulae' based on the effective medium theory, *J. Phys. D: Appl. Phys.* 31 (1998) 1589–1594.
- [24] J.A. Reynolds, J.M. Hough, Formulae for dielectric constant of mixtures, *Proc. Phys. Soc. Sec. B* 70 (8) (1957) 769–775.
- [25] J.C. Maxwell, *A Treatise on Electricity and Magnetism*, vol. 1, Clarendon Press, Oxford, UK, 1892.
- [26] Z. Hashin, Assessment of the self consistent scheme approximation: conductivity of particulate composites, *J. Compos. Mater.* 2 (3) (1968) 284–300.
- [27] J.D. Eshelby, The determination of the elastic field of an ellipsoidal inclusion, and related problems, *Proc. R. Soc. London, Ser. A Math. Phys. Sci.* 241 (1226) (1957) 376–396.
- [28] H. Hiroshi, T. Minoru, Equivalent inclusion method for steady state heat conduction in composites, *Int. J. Eng. Sci.* 24 (7) (1986) 1159–1172.
- [29] A.N. Norris, A.J. Callegari, P. Sheng, A generalized differential effective medium theory, *J. Mech. Phys. Solids* 33 (6) (1985) 525–543.
- [30] J.G. Berryman, Random close packing of hard spheres and disks, *Phys. Rev. A* 27 (2) (1983) 1053.
- [31] A. Kumar, T. Oey, S. Kim, D. Thomas, S. Badran, J. Li, F. Fernandes, N. Neithalath, G. Sant, Simple methods to estimate the influence of limestone fillers on reaction and property evolution in cementitious materials, *Cem. Concr. Compos.* 42 (2013) 20–29.
- [32] W. Ogoh, D. Groulx, Stefans problem: validation of a one-dimensional solid-liquid phase change heat transfer process, in: *COMSOL Conference*, Boston, United States, October 7–9, 2010.
- [33] H. Zhang, X. Wang, D. Wu, Silica encapsulation of *n*-octadecane via sol-gel process: a novel microencapsulated phase-change material with enhanced thermal conductivity and performance, *J. Colloid Interface Sci.* 343 (1) (2010) 246–255.
- [34] D. Zhang, A.S. Fung, O. Siddiqui, Numerical studies of integrated concrete with a solid-solid phase change material, in: *Second Canadian Solar Buildings Conference*, Calgary, Canada, June 10–14, 2007.
- [35] J.Z. Liang, F.H. Li, Measurement of thermal conductivity of hollow glass-bead-filled polypropylene composites, *Polym. Test.* 25 (4) (2006) 527–531.

- [36] J.Z. Liang, F.H. Li, Simulation of heat transfer in hollow-glass-bead-filled polypropylene composites by finite element method, *Polym. Test.* 26 (3) (2007) 419–424.
- [37] K.C. Yung, B.L. Zhu, T.M. Yue, C.S. Xie, Preparation and properties of hollow glass microsphere-filled epoxy-matrix composites, *Compos. Sci. Technol.* 69 (2) (2009) 260–264.
- [38] S.N. Patankar, Y.A. Kranov, Hollow glass microsphere HDPE composites for low energy sustainability, *Mater. Sci. Eng.: A* 527 (6) (2010) 1361–1366.
- [39] V.S. Shabde, K.A. Hoo, G.M. Gladysz, Experimental determination of the thermal conductivity of three-phase syntactic foams, *J. Mater. Sci.* 41 (13) (2006) 4061–4073.
- [40] T. Fiedler, E. Solórzano, A. Öchsner, Numerical and experimental analysis of the thermal conductivity of metallic hollow sphere structures, *Mater. Lett.* 62 (8) (2008) 1204–1207.